Neurobiology of Stress 13 (2020) 100258

Contents lists available at ScienceDirect

Neurobiology of Stress

journal homepage: www.elsevier.com/locate/ynstr

Optogenetically-induced long term depression in the rat orbitofrontal cortex ameliorates stress-induced reversal learning impairment

Samantha M. Adler [a], Milena Girotti [a], David A. Morilak [a,b,*]

[a] Department of Pharmacology and Center for Biomedical Neuroscience, UT Health San Antonio, 7703 Floyd Curl Dr, San Antonio, TX, 78229, USA
[b] South Texas Veterans Health Care System, San Antonio, TX, 78229, USA

ARTICLE INFO

Keywords:
Orbitofrontal cortex
Chronic stress
Plasticity
Optogenetics

ABSTRACT

Cognitive flexibility is a higher-order executive function that requires plasticity in neuronal circuits of the prefrontal cortex. Deficits in cognitive flexibility are prominent in a variety of psychiatric disorders, such as major depression, obsessive-compulsive disorder, and posttraumatic stress disorder. Chronic stress induces deficits in cognitive flexibility, perhaps through effects on plasticity, but the mechanism is not well understood. Previous work has demonstrated that stress reduces activity and dendritic elaboration in the medial prefrontal cortex (mPFC). In contrast, stress appears to increase dendritic elaboration in the orbitofrontal cortex (OFC). This suggests that there may be a differential effect of stress on plasticity in different prefrontal cortical areas. To test this hypothesis, we examined the effects of inducing plasticity optogenetically in the OFC on reversal learning, an OFC-mediated form of cognitive flexibility, in stressed and non-stressed rats. Inducing opto-LTD in the projection from mediodorsal thalamus to OFC ameliorated reversal learning deficits in rats exposed to chronic intermittent cold (CIC) stress. Additionally, we found that inducing opto-LTP in non-stressed rats produced deficits in reversal learning similar to those seen in rats after CIC stress. Finally, CIC stress produced complex subregion-specific changes in dendritic material and spine subtype composition in the OFC. These results indicate that the effects of stress on plasticity in the OFC are distinct from those in the mPFC, and that the PFC should therefore not be treated as a homogenous region in studying either stress effects or potential treatments for stress-related psychiatric disorders.

1. Introduction

Cognitive flexibility is the ability to modify previously established thoughts, patterns, or learned associations in order to adapt responding to changes in the environment. While deficits in cognitive flexibility are common in stress-related psychiatric disorders (Castaneda et al., 2008), treatment options rarely address this symptom dimension (Shilyansky et al., 2016). In some of these disorders, such as major depressive disorder, cognitive flexibility deficits are also thought to underlie the disorder's onset and maintenance (Beck, 2008). Stress exacerbates these symptoms and reduces cognitive flexibility in both humans (Raio et al., 2017) and rodents (Bondi et al., 2008).

Different forms of cognitive flexibility are mediated by different areas of the prefrontal cortex (PFC). For example, investigators using the attentional set-shifting test (AST), a rodent test that measures different components of cognitive flexibility (Birrell and Brown, 2000), showed that extradimensional set-shifting is mediated by the medial prefrontal cortex (mPFC), while reversal learning is mediated by the orbitofrontal cortex (OFC) (McAlonan and Brown, 2003). Also, different types of stressors produce different types of cognitive flexibility impairments: chronic unpredictable stress impairs set-shifting, while chronic intermittent cold stress (CIC) impairs reversal learning (Bondi et al., 2008; Danet et al., 2010). Therefore, it is possible to manipulate one form of cognitive flexibility while leaving the other intact, letting us further elucidate the behavioral role of each subregion.

Previous studies have reported that the mPFC has reduced activity in depressed humans as compared to controls when measured with PET imaging (Baxter et al., 1989). This has been supported by rodent studies indicating that chronic stress causes a decrease in dendritic length (Liston et al., 2006). Additional studies have demonstrated that ketamine, a novel and rapid-acting antidepressant, has the opposite effect, causing an increase in dendritic length and spine density in the mPFC (Li

* Corresponding author. Department of Pharmacology and Center for Biomedical Neuroscience, UT Health San Antonio, 7703 Floyd Curl Dr, San Antonio, TX, 78229, USA.
E-mail address: morilak@uthscsa.edu (D.A. Morilak).

https://doi.org/10.1016/j.ynstr.2020.100258
Received 5 June 2020; Received in revised form 12 October 2020; Accepted 15 October 2020
Available online 24 October 2020

et al., 2010).

Evidence suggests that the OFC may behave in an opposite manner, pointing to a unique role of this brain region in stress-related pathology. Human imaging studies demonstrate that OFC has increased activity in patients with depression, and that this is corrected after antidepressant treatment (Drevets, 2000). Additionally, previous work has demonstrated that chronic restraint stress in rats increases dendritic length in the OFC (Liston et al., 2006). Finally, our lab has previously demonstrated that ketamine, which attenuates the detrimental effects of chronic intermittent cold stress on reversal learning, produces an attenuation of electrical responses evoked in the OFC by stimulation of the afferent from the mediodorsal thalamus (MDT) (Patton et al., 2017). Together, this indicates that an increase in activity in the OFC may underlie stress-induced reversal learning deficits.

We thus wanted to determine if directly inducing long term depression (LTD) in the MDT to OFC afferent pathway could reduce the negative effects of stress on reversal learning, mimicking the beneficial effects of ketamine on cognitive flexibility. Using virally-mediated expression of the ChETA variant of channelrhodopsin driven by a CamKIIα promoter, we selectively activated the afferent glutamatergic MDT-OFC pathway. After confirming our ability to optically induce LTD-like plasticity in the OFC, we tested the behavioral effects of opto-LTD on reversal learning. Using a similar approach, we then wanted to determine if optically inducing long term potentiation (LTP) in the MDT-OFC pathway would be sufficient to mimic the effects of CIC on reversal learning. Finally, we examined if stress produced changes in neuronal structure in the OFC that may underlie CIC stress-induced reversal learning deficits. Portions of this work have been presented in abstract form (Adler et al., 2018, 2019).

2. Materials and methods

A total of 142 male and 131 female adult Sprague Dawley rats (Envigo) weighing 225 g–249 g upon arrival were used in these studies. All rats were housed in a 12/12 h light/dark cycle (lights on at 0700 h) with *ad libitum* food and water, except for the period of food restriction prior to reversal learning testing. Prior to experimentation, rats were singly housed. All procedures were in accordance with National Institutes of Health guidelines and approved by the University of Texas Health Science Center at San Antonio Institutional Animal Care and Use Committee.

2.1. Viral injection of ChETA or GFP constructs

We injected an AAV5 viral vector to deliver a construct encoding ChETA, a blue light-sensitive channelrhodopsin with rapid temporal kinetics (Gunaydin et al., 2010), bilaterally into the MDT. A separate group of animals received a GFP control construct. These constructs were driven by a CamKIIα promoter to allow selective expression in glutamatergic neurons. For viral injection, rats were placed in a stereotaxic frame while under isoflurane anesthesia. Microinjectors were lowered into the MDT (AP -2.5 mm, ML ±0.9 mm, DV -5.1 mm from Bregma). Each side received 0.5 μL of AAV5-CaMKIIα-ChETA-YFP or control AAV5-CaMKIIα-GFP virus (3×10^9 viral particles/μL, UPenn Vector Core obtained through Addgene, Watertown, MA). After the injection, microinjectors remained in place for 10 min to allow diffusion. For rats undergoing reversal learning testing, dual fiber optic cannulae (Doric Lenses, Quebec, Canada) were implanted bilaterally 1 mm above the orbitofrontal cortex (OFC) (AP +2.9 mm, ML ±2.6 mm, DV -4.2 mm). The implant was secured to the skull using super glue, jeweler's screws, and dental cement.

2.2. Electrophysiology

In vivo electrophysiology was used to measure changes in evoked local field potentials by stimulating in the MDT and recording in the OFC. Four to six weeks after viral injection, rats were anesthetized with chloral hydrate (400 mg/kg, i. p.) and then placed in a stereotaxic frame. A bipolar platinum electrode was lowered in either the left or right MDT (AP -2.5 mm, ML ±0.9 mm, DV -5.4 mm from Bregma). A custom-made probe with an optical fiber affixed to and terminating 1 mm above the tip of a tungsten recording electrode (Doric Lenses) was then placed above the ipsilateral OFC (AP +2.9 mm, ML ±2.6 mm, DV -4.2±1 mm). The optical fiber was connected to a 473 nm solid-state laser diode (OptoEngine, Midvale, UT) with 13–15 mW output. After 15–30 min of acclimation, evoked responses were recorded (low cutoff filter 0.3 Hz, high cutoff 1000 Hz) and digitized (Power Lab; ADInstruments, Colorado Springs, CO). Stimulus-response curves were generated by recording responses evoked in the OFC by stimulating the MDT (260 μs pulse width, 0.1 Hz, 100–1000 μA in 100 μA increments). Response amplitude was measured from the first negative deflection peak (N1), which occurs 5±3 ms after stimulation, to the first positive deflection peak (P1), which occurs 18±3 ms after stimulation. Traces were averaged per minute, recording for 5 min at each stimulus intensity. For LTD and LTP experiments, stimulus intensity was set to elicit a response of 50%–75% of maximum. Baseline responses were then recorded over 15 min, with traces averaged per minute. After the baseline, rats received optical blue laser light stimulation of MDT terminals in the OFC. Optical stimulation parameters were derived initially from electrical stimulation parameters used to induce LTD and LTP in the MDT projection to mouse medial prefrontal cortex (Herry and Garcia, 2002), then adapted to induce opto-LTD and opto-LTP in the rat mPFC (Bulin et al., 2020). Opto-LTD was induced using 900 light pulses with a 2 ms pulse width delivered at 1 Hz over the course of 15 min. Opto-LTP was induced using 10×1s trains of light pulses with a 1 ms pulse width delivered at 250 Hz once every 10 s. After inducing either opto-LTD or opto-LTP, electrical stimulation was then resumed for the remainder of a 3-h recording period. After the experiment, electrode placement was analyzed and 6 rats with incorrect electrode placement were excluded from analysis. Mean baseline was calculated as the average across the 15-minute baseline period. Response amplitude during minutes 100 to 160 of the recording session was calculated as a percentage of the mean baseline and was reported as the post-stimulation value. Fig. 1C and D shows electrode placements for the opto-LTD and opto-LTP experiments, respectively.

2.3. Chronic intermittent cold stress

Chronic intermittent cold stress was conducted as described previously (Lapiz-Bluhm et al., 2009). Rats individually housed in their home cage were placed in a 4 °C room for 6 h each day during the light portion of the cycle and then returned to housing over a period of 14 consecutive days. Control animals remained in their original housing room.

2.4. Reversal learning test

Rats were tested on reversal learning as described previously (Donegan et al., 2014). Animals were food restricted starting 7 days prior to testing, to 11 g per day for males and 7 g per day for females. Animals were trained to dig in terracotta pots baited with a reward of ½ of a Honey Nut Cheerio (General Mills Cereals, Minneapolis, MN) buried in the bottom 1/3 of the pot. Each pot utilized two stimulus dimensions: a medium that filled the pot and a scent that was applied to the rim of the pot using aromatic oil (Frontier Natural Brands, Norway, IA). During the first two days after the end of CIC, rats were trained to perform the task. Testing took place three days after the end of CIC. On testing day, the rat first performed a simple discrimination, where only one dimension was used (for example, odor). Then, the rat was tested in a compound-discrimination, where the distracting irrelevant dimension was introduced (for example, different digging media). Finally, the rat underwent reversal learning, where the rewarding stimulus was swapped (for example, if clove was the rewarded scent and nutmeg was

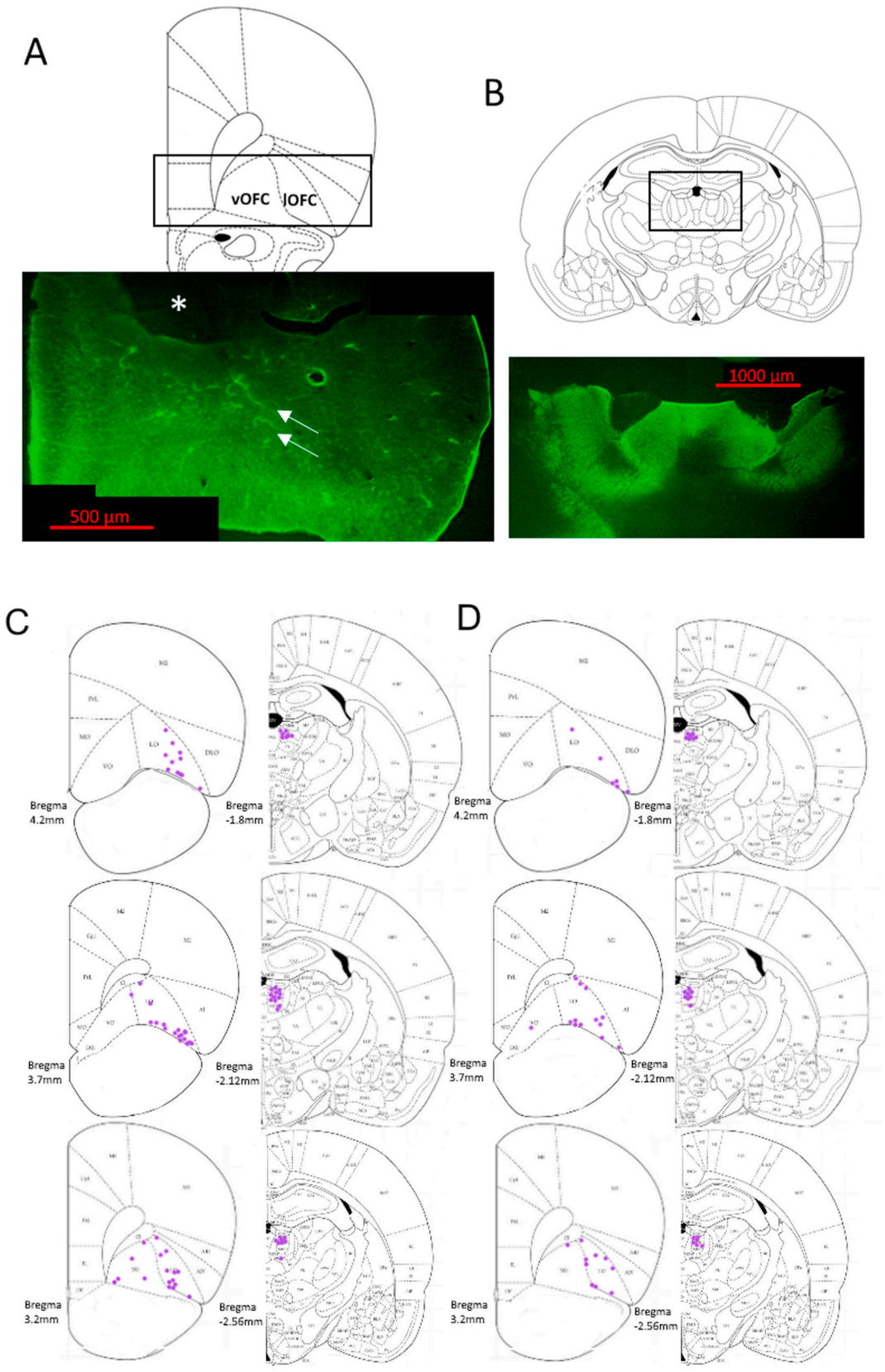

Fig. 1. Demonstration of viral expression and electrode placement for electrophysiology experiments. A. Representative image of AAV5-CamKIIα-ChETA terminal expression in the OFC 6 weeks after injection. * indicates the track of the OFC opto-probe. Arrows highlight ChETA-containing terminals. Scale bar = 500 µm. **B.** Representative image of AAV5-CamKIIα-ChETA expression at the bilateral injection sites in the MDT after 6 weeks. Scale bar = 1000 µm. **C.** Recording electrode placement in OFC (left) and stimulating electrode placement in MDT (right) for opto-LTD experiments. **D.** Recording electrode placement in OFC (left) and stimulating electrode placement in MDT (right) for opto-LTP experiments.

unrewarded, the contingency was switched so that nutmeg was rewarded). In each stage, six correct trials in a row were required before moving on to the next stage. The total number of trials to complete each stage was recorded as the trials to criterion. If no choice was made during the 10-minute trial length, a response of "no choice" was given and the trial was omitted. Rats "failed out" if they had six "no choice" responses recorded in a row; one rat was removed from the study for this reason. Three rats were excluded because testing had not completed before the onset of the dark cycle. Five rats were removed from the study because their head caps were dislodged prior to the completion of the laser stimulation protocol.

2.5. Experiment 1. Effect of opto-LTD on reversal learning

Four weeks after viral injections and fiber optic cannulae surgeries, rats (45 males, 41 females) were subjected to CIC stress or left undisturbed in their home cages for a period of 14 days and then trained for the reversal test. Immediately after the compound discrimination phase of testing, animals were laser stimulated for a 15-minute LTD protocol and then left in their home cage for the remainder of a 1-h period before resuming the behavioral test to completion of the reversal stage.

2.6. Experiment 2. Effect of opto-LTP on reversal learning

Rats (24 males, 22 females) were injected with virus and implanted with optic fibers aimed at the OFC. CIC stress was not administered in this experiment. Four to six weeks after surgery the rats were trained for the reversal test. Immediately after the compound discrimination phase of testing, animals underwent a 90 s LTP protocol and then were left in their home cage for the remainder of a 1-h period before testing resumed on the reversal learning task.

2.7. Immunohistochemistry

We utilized immunohistochemistry to confirm ChETA expression at the MDT injection site and in OFC terminals. Rats were sacrificed via rapid decapitation after reversal learning testing and brains were placed in 4% paraformaldehyde. Then, 40 μm brains slices containing the OFC and MDT were obtained for free-floating immunohistochemistry. After inactivation of endogenous peroxidases using hydrogen peroxide, sections were placed in a primary rabbit anti-GFP antibody (1:5000; Cell Signaling, Danvers, MA, Cat#2555) at 4 °C overnight. The next day, sections were incubated with an anti-rabbit IgG HRP-linked antibody (1:1000; Cell Signaling, Cat #7074), reacted with fluorescein-conjugated tyramide (TSA-Plus, PerkinElmer, Waltham, MA) and then counterstained with DAPI. Fig. 1A and B shows representative images of ChETA-GFP expression in OFC and MDT, respectively.

2.8. DiOlistic labelling

A separate cohort of rats were lightly perfused using 1.5% paraformaldehyde. Then, we collected 200 μm brain slices for DiOlistic labelling. To label neurons, DiI-coated gold particles (1.6 μm) were delivered ballistically into the brain section with a gene gun (BioRad). Slices were incubated in 1X PBS overnight in the dark at room temperature to allow the dye to spread throughout neurons contacted by the particles. The next day, slices were mounted and coverslipped using Fluoromount (Sigma-Aldrich, St. Louis, MO). Slices were optically sectioned and images acquired on a Zeiss Axio Observer.Z1 inverted microscope equipped with an Apotome.2 structured illumination module within one week to avoid the dye fading or leaching out of the membrane. The experimenter was blind to treatment group during subsequent analysis.

For Sholl analysis, images were obtained at 20x, traced in Neurolucida 360, and analyzed in Neurolucida Explorer. Concentric rings were spaced 10 μm apart and starting 10 μm away from the cell body. An average of 7.2 ± 1.0 cells were analyzed in each brain (an average of 3.1 cells per brain in medial OFC (mOFC), 2.4 in ventral OFC (vOFC) and 3.0 in lateral OFC (lOFC)). Within each region, data from all cells in a given brain were averaged so that each rat represented a single case in the group analyses. For analysis, the dendritic arbors were divided into thirds based upon each neuron's maximal extent, and the amount of dendritic material was assessed in proximal, middle, and distal segments.

To determine spine density, images of the apical dendrite were acquired using a Plan-Apochromat 63x/1.4 oil objective. One segment was selected every 50 μm throughout the length of the apical dendrite using Neurolucida 360. For each segment, the spine density was calculated, and then the density of segments were averaged for each neuron. Each subregion was analyzed separately. Proximal and distal segments were also analyzed separately: proximal segments were classified as those at distances less than 150 μm from the cell body, while segments at distances greater than 150 μm were classified as distal. An average of 6.1 ± 0.7 cells were analyzed in each brain (an average of 2.2 cells per brain in mOFC, 2.3 in vOFC and 2.6 in lOFC). Within each region, data from all cells in a given brain were averaged so that each rat represented a single case in the group analyses. Each subtype classification and OFC subregion were analyzed separately.

2.9. Data analysis

Data were analyzed using one-, two-, or three-way ANOVA using GraphPad Prism (GraphPad Software), including sex as a factor. When no significant sex differences were found, males and females were combined within groups for analysis by *t*-test, one-way ANOVA, or two-way ANOVA. Pairwise comparisons to detect group differences were analyzed using the Holm-Sidak test. Significance was determined at $p < 0.05$. Experiments were not powered to explicitly test for sex differences. Nonetheless, as per NIH requirements, data are still shown for both sexes separately, and sex was included as a factor in the initial analyses. Evoked potentials were analyzed using nonlinear regression and then compared by Least-Sums-of-Squares *F* Test. Pairwise comparisons were conducted to determine the effects of stress and sex using *post hoc* analyses and applying the Bonferroni correction for multiple comparisons.

3. Results

3.1. Establishing optically-induced plasticity in the MDT-OFC pathway

In order to investigate how LTD or LTP induction in the OFC influences reversal learning, we first needed to establish that we were able to induce LTD and LTP in the OFC using the optogenetic ChETA virus. To this end, we performed *in vivo* anesthetized recordings of evoked local field potentials by placing a stimulating electrode in the MDT and dual recording electrode and optical fiber in the OFC (Fig. 1C and D).

Because no sex difference was detected in the opto-LTD induction experiment ($F_{(1,39)} = 0.9510$, $p = 0.3355$), we combined males and females within groups. In non-stressed rats harboring the ChETA virus and receiving opto-LTD (Fig. 2A–C), the magnitude of the evoked field potentials was 81.6% of baseline, significantly lower than in the GFP control group (repeated-measures ANOVA, $F_{(2,37)} = 10.13$, $p = 0.0003$). Stimulation using the opto-LTD protocol in rats that received only the GFP control virus produced no change in evoked response (103.1% of baseline), demonstrating that the laser itself did not cause a depressed response. Additionally, rats that underwent CIC also experienced a reduction in evoked field potential response after opto-LTD induction (70.7% of baseline), indicating that stress did not interfere with ChETA functionality or the induction of LTD. For simplicity of presentation and comparison, the mean relative response amplitudes during minutes 100–160, at which time any post-stimulation decrease had stabilized, were calculated and compared. These comparisons are shown in Fig. 2A, D, and E. Results are shown separately by sex in Fig. 2D and E.

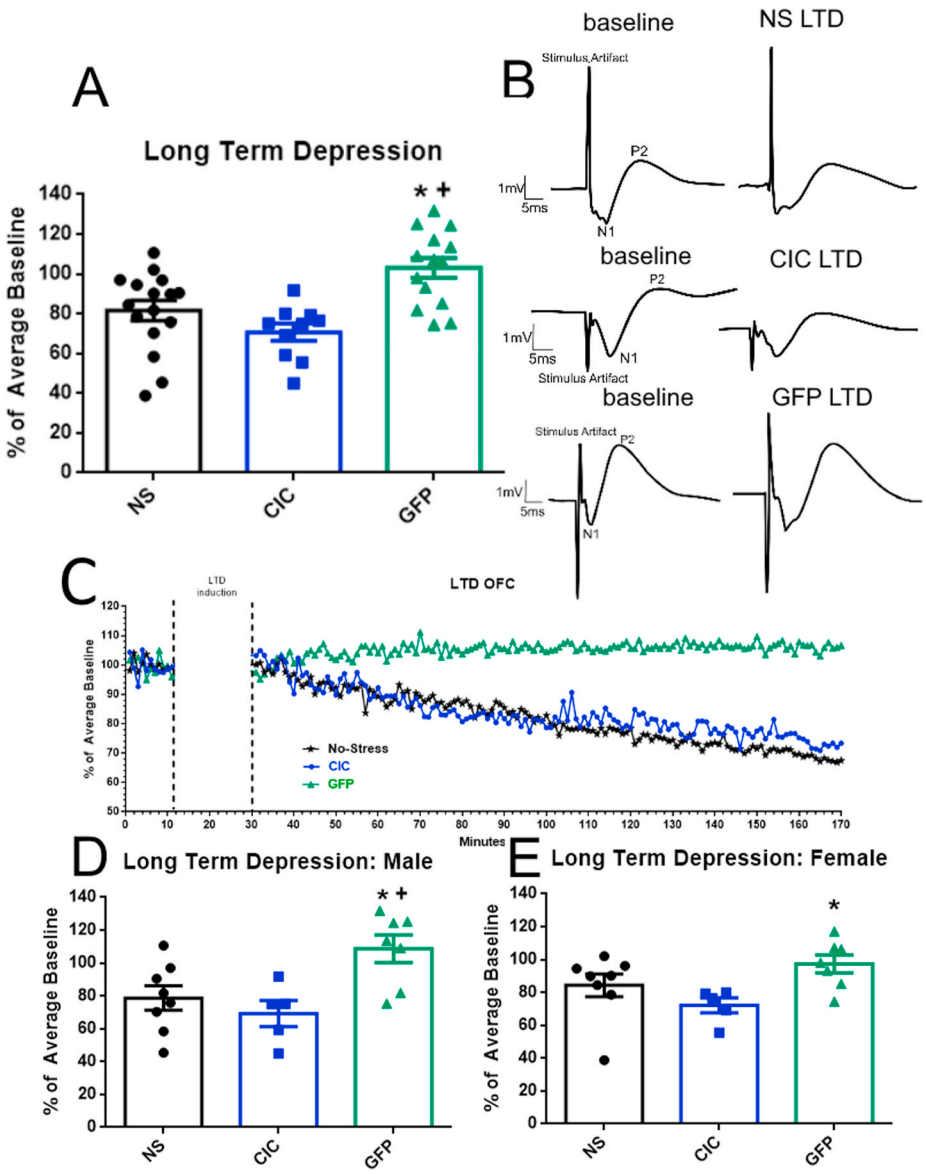

Fig. 2. Optical induction of LTD in the MDT-OFC pathway. A. Optical induction of LTD in the OFC of non-stressed control rats that received ChETA virus (NS) demonstrate a decrease in evoked response compared to GFP control rats (GFP). Each point is the average post-stimulation value for each recorded animal (n = 10–17 per group). Rats undergoing cold stress (CIC) are just as sensitive to opto-LTD stimulation as non-stressed rats. *p < 0.01 compared to non-stressed animals; +p < 0.001 compared to cold-stressed animals. One point was excluded due to the Grubbs Outlier Test. **B.** Representative traces of each group before laser stimulation (left) and 120–140 min after laser stimulation (right). **C.** Representative graphs of evoked LFP response over time after opto-LTD stimulation. **D.** Results in male rats (n = 5–8 per group). *p < 0.05 compared to non-stressed animals; + p < 0.05 compared to cold-stressed animals. **E.** Results in female rats (n = 5–8 per group); *p < 0.05 compared to cold-stressed animals.

Because no sex difference was detected in the opto-LTP induction experiment ($F_{(1,42)} = 2.833$, $p = 0.0998$), we combined males and females within groups. In non-stressed rats harboring the ChETA virus receiving opto-LTP (Fig. 3A–C), the magnitude of evoked field potentials averaged 111.6% of baseline, which was significantly higher than the GFP control group (90.2%) (repeated-measures ANOVA, $F_{(2,63)} = 5.038$, $p = 0.0093$; Fig. 3A). Rats that underwent CIC stress showed no increase in response after optically-induced LTP (93.3% of baseline), significantly different from the non-stressed group ($p < 0.05$ Fig. 3A), indicating occlusion of LTP. This suggests that similar mechanisms may be involved in CIC stress-induced potentiation and optically-induced potentiation of evoked responses. As above, the mean relative response amplitudes during minutes 100–160, at which time any post-stimulation increase had stabilized, were calculated and compared. These comparisons are shown in Fig. 3A, D, and E. Results are shown separately by sex in Fig. 3D and E.

3.2. LTD induction in the OFC rescues a CIC-induced deficit in reversal learning

To test if reduction of the afferent-evoked response in the MDT-OFC pathway can attenuate a stress-induced deficit in reversal learning, we performed opto-LTD in CIC stressed rats (Fig. 4A shows a diagram of the timeline). In the initial analysis, there was no effect of sex ($F_{(1,70)} = 0.0384$, $p = 0.8578$). Rats had impaired performance in reversal after CIC, and opto-LTD induction rescued this deficit (Stress × Treatment interaction, $F_{(1,68)} = 12.85$, $p = 0.0006$; Treatment, $F_{(1,68)} = 0.5342$, $p = 0.4673$; Stress, $F_{(1,68)} = 0.003356$, $p = 0.9540$; Fig. 4B). The non-stressed control groups consisted of rats injected with GFP instead of ChETA and rats that received the active ChETA virus but no laser stimulation. These groups were combined after a *t*-test revealed no significant difference between these two control conditions ($p = 0.7114$). Results are shown separately by sex in Fig. 4C and D.

To test for regional specificity, we induced opto-LTD in the MDT to mPFC pathway, as described previously (Bulin et al., 2020). Whereas inducing opto-LTD in the MDT-OFC pathway improved performance in CIC-stressed rats, stressed rats receiving opto-LTD in the MDT-mPFC pathway did not perform any better than stressed no-laser control rats. This indicates that the facilitating behavioral effect of opto-LTD on reversal learning after CIC stress is specific to the MDT-OFC pathway ($F_{(2,37)} = 9.046$, $p < 0.001$; Fig. 4E). These results are shown separately by sex in Fig. 4F and G.

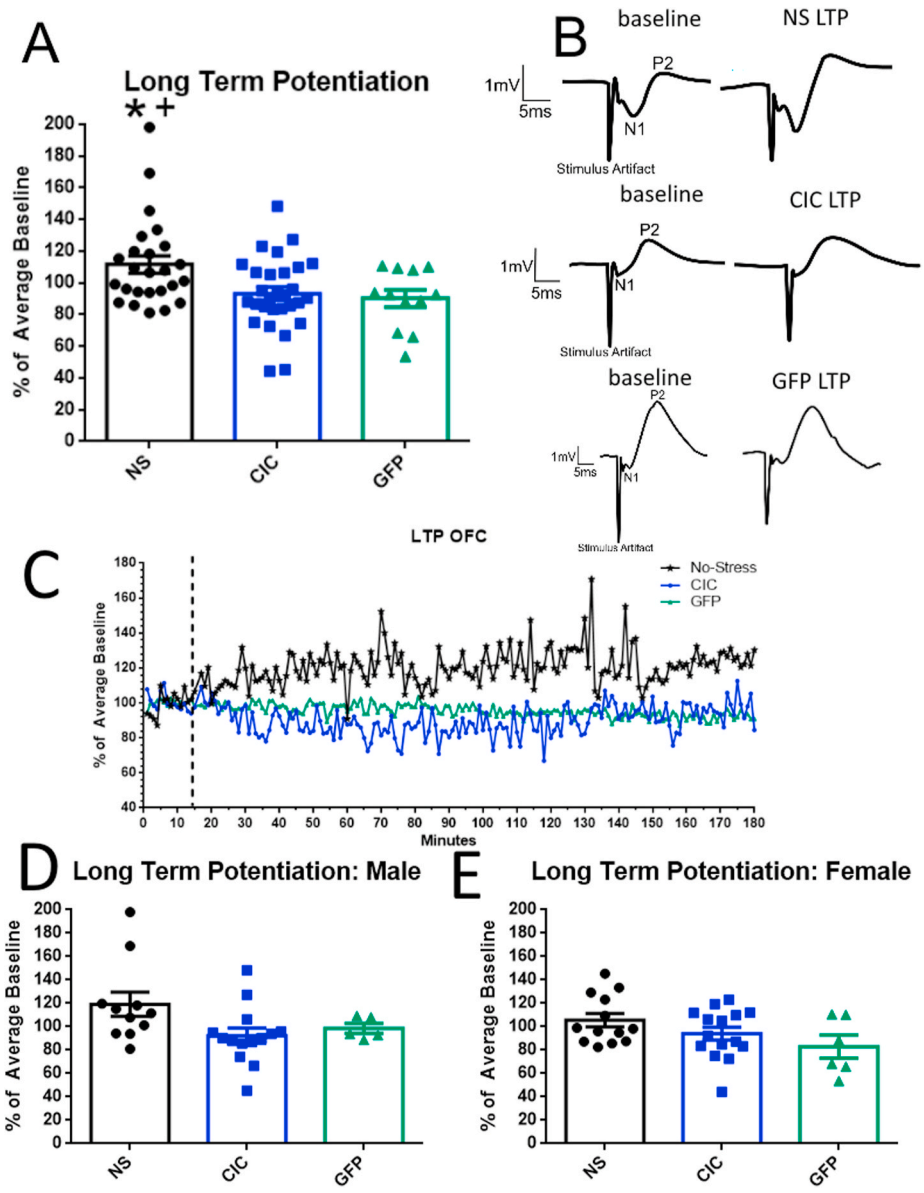

Fig. 3. Optical induction of LTP in the MDT-OFC pathway A. Optical induction of LTP in the OFC of rats that received ChETA virus demonstrates an increase in evoked response compared to GFP control rats. Each point is the average post-stimulation value for each recorded animal (n = 12–29 per group). Rats undergoing cold stress appear to exhibit an occlusion of LTP induction. *p < 0.05 compared to cold-stressed animals; + p < 0.05 compared to GFP control animals. One point was excluded due to the Grubbs Outlier Test. **B.** Representative traces of each group before laser stimulation (left) and 130–150 min after laser stimulation (right). **C.** Representative graphs of evoked LFP response over time after opto-LTP stimulation. **D.** Results in male rats (n = 6–15 per group). One point was excluded due to the Grubbs Outlier Test. **E.** Results in female rats (n = 13–15 per group).

3.3. LTP induction in the OFC mimics the effects of CIC stress on reversal learning

We next tested if potentiation of the MDT-OFC pathway can mimic a stress-induced deficit in reversal learning (Fig. 5A). In the initial analysis, there was no effect of sex ($F_{(1,36)} = 0.01745$, $p = 0.8956$). Rats with active ChETA virus that underwent opto-LTP stimulation performed worse in the reversal learning phase of the task than all other groups (Laser × Virus interaction, $F_{(1,40)} = 4.275$, $p = 0.0452$; Laser $F_{(1,40)} = 3.754$, $p = 0.0598$; Virus $F_{(1,40)} = 3.507$, $p = 0.0687$; Fig. 5B). Results are shown separately by sex in Fig. 5C and D.

Additionally, in a separate experiment to test regional specificity, we induced opto-LTP in the MDT pathway to mPFC, as described previously (Bulin et al., 2020). We found that rats receiving opto-LTP in the MDT-mPFC pathway do not perform any differently than the no-laser control group, but are significantly different from the rats that received opto-LTP in the MDT-OFC pathway, indicating that this effect is specific to the OFC ($F_{(2,30)} = 7.865$; $p = 0.0018$, Fig. 5E). These results are shown separately by sex in Fig. 5F and G.

3.4. Analysis of dendritic length and spines in the orbitofrontal cortex

Finally, we aimed to elucidate how chronic stress alters neuronal morphology in the orbitofrontal cortex using DiOlistic labelling (Fig. 6). Fig. 6A shows a representative image of a traced neuron. Fig. 6B shows different subtypes of spines identified in this experiment and Fig. 6C shows the distribution of the labeled neurons throughout the OFC. First, we compared dendritic length using Sholl analysis. In the OFC overall (Fig. 7A, n = 8–11 per group), there was a significant effect of the interaction between stress and radial distance from the soma ($F_{(45,765)} = 1.585$; $p = 0.0097$), as well as a main effect of radial distance ($F_{(45,765)} = 170.5$; $p < 0.0001$), but not a significant effect of stress alone ($F_{(1,17)} = 0.7968$, $p = 0.3845$). When the dendritic tree was analyzed in proximal, middle and distal segments, there were not any significant differences between stressed and non-stressed animals at any of the individual segment areas in the OFC as a whole (Fig. 7B). Likewise, there was no difference in total dendritic material or branch nodes in the OFC or in any of its subregions (Supplemental Fig. S1).

However, analyses of the OFC subregions separately revealed striking differences between them. In the mOFC (n = 7 per group), we found a main effect of radial distance ($F_{(45,540)} = 109.7$; $p < 0.0001$, Fig. 7C) as

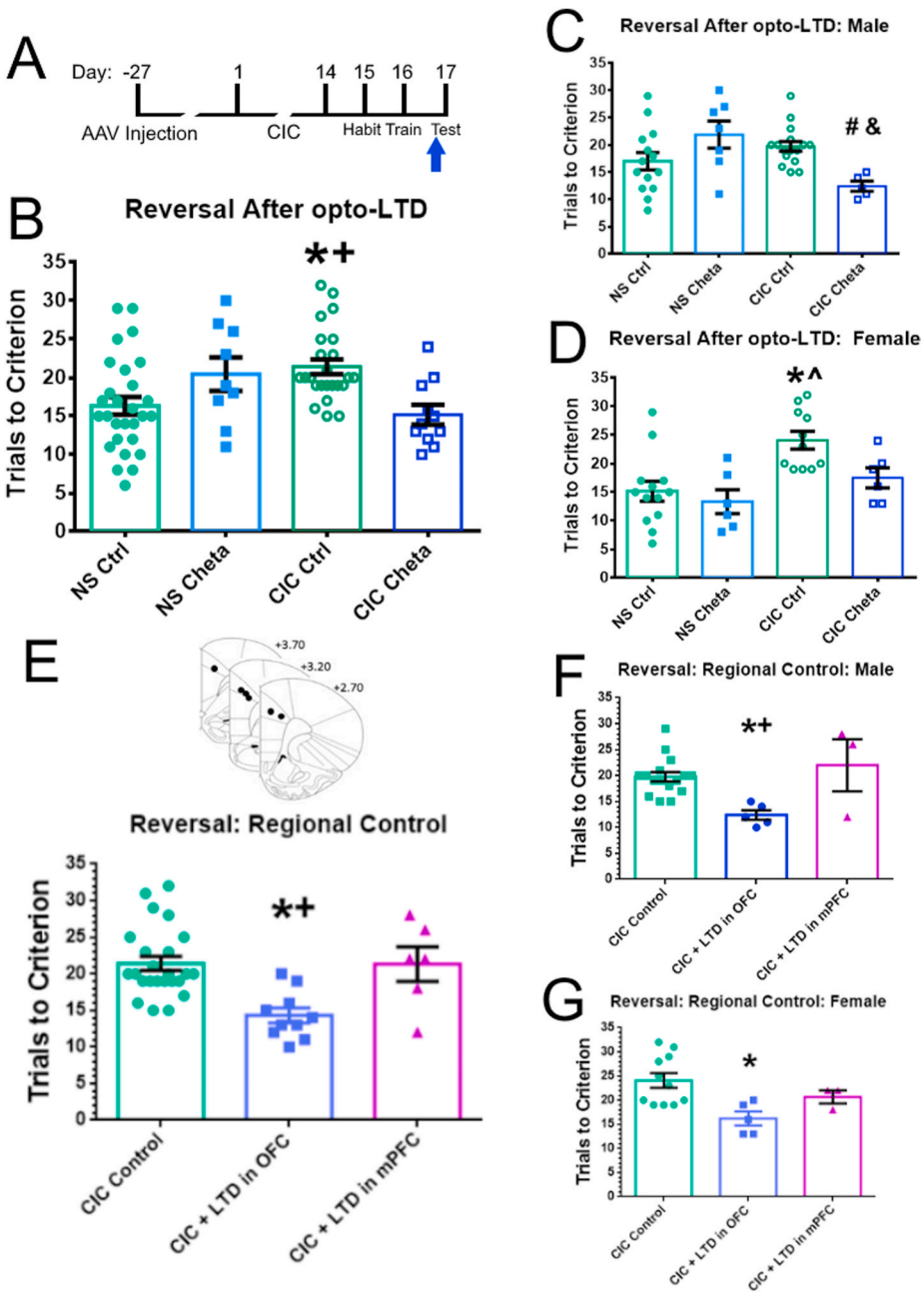

Fig. 4. Opto-LTD in the MDT-OFC pathway rescues a cold-stress-induced deficit in reversal learning. A. Experimental timeline for opto-LTD experiments. Blue arrow indicates opto-LTD stimulation 1 h before reversal learning. **B.** Opto-LTD was induced 1 h prior to reversal learning (n = 9–28 per group). Rats that underwent CIC performed significantly worse at reversal learning. Opto-LTD induction in CIC-stressed rats with active ChETA virus attenuated this deficit. The control group (NS-Ctrl) includes both rats injected with GFP control virus as well as rats that received ChETA virus without laser stimulation. NS-ChETA represents non-stressed rats expressing ChETA and undergoing laser stimulation. *p < 0.01 compared to non-stressed controls, +p < 0.05 compared to cold-stressed animals with ChETA and laser stimulation. **C.** Results in male rats (n = 5–16 per group). #p < 0.05 compared to cold-stressed controls, &p < 0.05 compared to non-stressed animals with ChETA and laser stimulation. **D.** Results in female rats (n = 6–13 per group). *p < 0.05 compared to non-stressed controls, ^p < 0.05 compared to non-stressed animals with ChETA and laser stimulation. **E.** Results of optically-induced plasticity in the medial prefrontal cortex to test pathway specificity (n = 6–24 per group). CIC-stressed rats receiving opto-LTD induction in the mPFC still had deficits in reversal learning. *p < 0.005 compared to cold-stressed control animals, +p < 0.05 compared to animals that received CIC + LTD in the mPFC. Inset shows the localization of the tips of the optical fibers, implanted 1 mm above the target in mPFC. Fibers were implanted bilaterally, but for clarity, tip localization is mapped on one side only. **F.** Results in male rats (n = 3–16 per group). *p < 0.01 compared to cold-stressed control animals, +p < 0.01 compared to animals that received CIC + LTD in the mPFC. **G.** Results in female rats (n = 3–11 per group). *p < 0.05 compared to cold-stressed control animals. (For interpretation of the references to colour in this figure legend, the reader is referred to the Web version of this article.)

well as a significant interaction between stress and radial distance ($F_{(45,540)} = 1.746$, $p = 0.0025$, Fig. 7C), but no effect of stress alone ($F_{(1,12)} = 0.05332$, $p = 0.8213$). Analysis of the separate segments of the dendritic tree revealed a significant increase in dendritic length in the middle segment in stressed rats accompanied by a near-significant increase at the distal segment (Fig. 7D). In the ventral OFC (Fig. 7E, n = 8–10 per group) there was a significant main effect of radial distance ($F_{(39,624)} = 101.1$, $p < 0.001$) but no significant main effect of stress ($F_{(1,16)} = 0.08373$, $p = 0.7760$) or significant interaction between the two ($F_{(39,624)} = 0.73038$, $p > 0.9999$). There was no significant effect of stress on dendritic morphology in any dendritic segment (Fig. 7F). In the lOFC (Fig. 7G, n = 6–11 per group), there was a main effect of radial distance ($F_{(35,595)} = 108.2$; $p < 0.0001$) and a significant interaction between stress and radial distance ($F_{(35,595)} = 2.557$, $p < 0.0001$, Fig. 7G) but no effect of stress alone ($F_{(1,17)} = 3.162$, $p = 0.0932$). The middle segment of the lOFC behaves in the opposite manner to the mOFC, demonstrating a significant decrease in dendritic length in stressed rats (Fig. 7H). For Sholl analysis stratified by sex, see Supplemental Fig. S2.

Finally, we used DiOlistic labelling to compare spine density and spine type composition between stressed and non-stressed rats. There are no significant differences in total apical spine density in any of the OFC subregions, or in the OFC as a whole (Supplemental Figs. S3A and S3B). This is consistent for both proximal (<150 μm) (Figs. S3C and S3D) and distal (>150 μm) (Figs. S3E and S3F) regions of the apical dendrite.

However, there were changes in specific spine subtypes. For a summary of the effects of CIC stress on spine subtypes, see Table 1. For a summary of the effects of sex on spine subtypes, see Table 2. With regard to the OFC as a whole, there was a significant effect of stress to decrease the number of filopodia in the overall OFC ($p < 0.05$, *t*-test, Supplemental Fig. S4A). There was also a significant effect of sex on the percentage of thin spines in the overall OFC ($F_{(1,16)} = 5.554$, $p = 0.0315$, Supplemental Fig. S4B), but no effect of stress ($F_{(1,16)} = 0.7616$, $p = 0.3957$) and no interaction between stress and sex ($F_{(1,16)} = 0.009942$, p

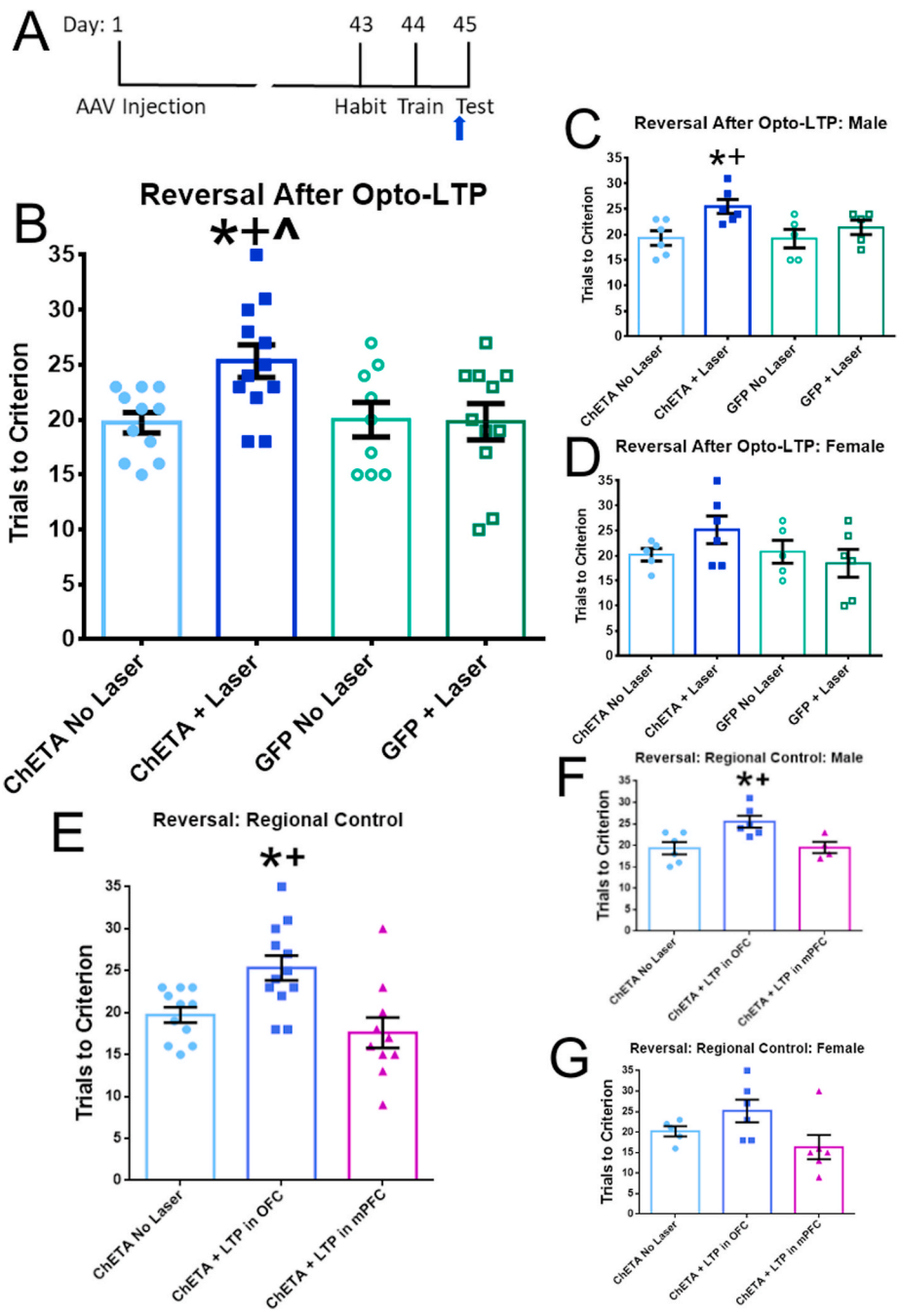

Fig. 5. Opto-LTP in the MDT-OFC pathway mimics a cold-stress-induced deficit in reversal learning. A. Experimental timeline for opto-LTP experiments. Blue arrow indicates opto-LTP stimulation 1 h before reversal learning. **B.** Opto-LTP was induced 1 h prior to reversal learning (n = 9–12 per group). Rats that had the active ChETA virus performed significantly worse at reversal learning. *p < 0.05 compared to animals with ChETA virus but no laser stimulation, +p < 0.05 compared to animals with inactive GFP virus and no laser stimulation, ^p < 0.05 compared to inactive GFP virus with laser stimulation. **C.** Results in male rats (n = 5–6 per group). *p < 0.05 compared to animals with ChETA virus but no laser stimulation, +p < 0.05 compared to animals with inactive GFP virus and no laser stimulation. **D.** Results in female rats (n = 5–6 per group). No significant post-hoc comparisons were observed in this group. **E.** Again, we conducted a regional specificity experiment with laser stimulation in the mPFC (n = 10–12 per group). Rats receiving opto-LTP laser stimulation in the mPFC did not have deficits in reversal learning. *p < 0.05 compared to ChETA No Laser, +p < 0.01 versus LTP in mPFC. **F.** Results in male rats (n = 4–6 per group). *p < 0.05 compared to ChETA No Laser, +p < 0.05 versus LTP in mPFC. **G.** Results in female rats (n = 5–6 per group). No significant post-hoc comparisons were observed in this group. (For interpretation of the references to colour in this figure legend, the reader is referred to the Web version of this article.)

= 0.9218).

In the medial OFC, almost every spine subtype was affected. Stress increased the proportion of thin spines and decreased the proportion of mushroom spines and filopodia ($p < 0.05$, *t*-test, Supplemental Fig. S4C). Additionally, there were more mushroom spines in non-stressed male rats than in any other group when analyzed by sex ($p < 0.05$, Supplemental Fig. S4D), and there are more filopodia in non-stressed male rats than in stressed females ($p < 0.05$, Supplemental Fig. S4D). There was also a significant effect of sex ($F_{(1,13)} = 15.53$, $p = 0.0017$), stress ($F_{(1,13)} = 22.77$, $p = 0.0004$), and the interaction between sex and stress ($F_{(1,13)} = 5.501$, $p = 0.0355$) on mushroom spines in the mOFC. Together, these data may indicate a shift away from mushroom spines towards thin spines and filopodia after CIC stress in the medial OFC.

Stress also reduced filopodia in the ventral OFC to a near-significant degree ($p = 0.05$, Supplemental Fig. S4E). There were no effects of stress on spine subtypes in the ventral OFC (Supplemental Fig. S4F). The effect of stress on filopodia was only absent in the lateral subregion of the OFC (Fig. S4G), likely due to the very low percentage of filopodia in this region (typically less than 6%). There were also no sex effects on spine subtypes in the lateral OFC (Supplemental Fig. S4H).

4. Discussion

LTP and LTD describe activity-dependent functional and structural plasticity in excitatory synaptic transmission (Lüscher et al., 2000; Malenka and Bear, 2004). As such, these terms are most strictly used to define changes in the magnitude of mEPSCs, and the responses measured in the present study are most appropriately described as "LTP-like potentiation and LTD-like attenuation of evoked local field potentials". Therefore, it is important to clarify that we use the terms

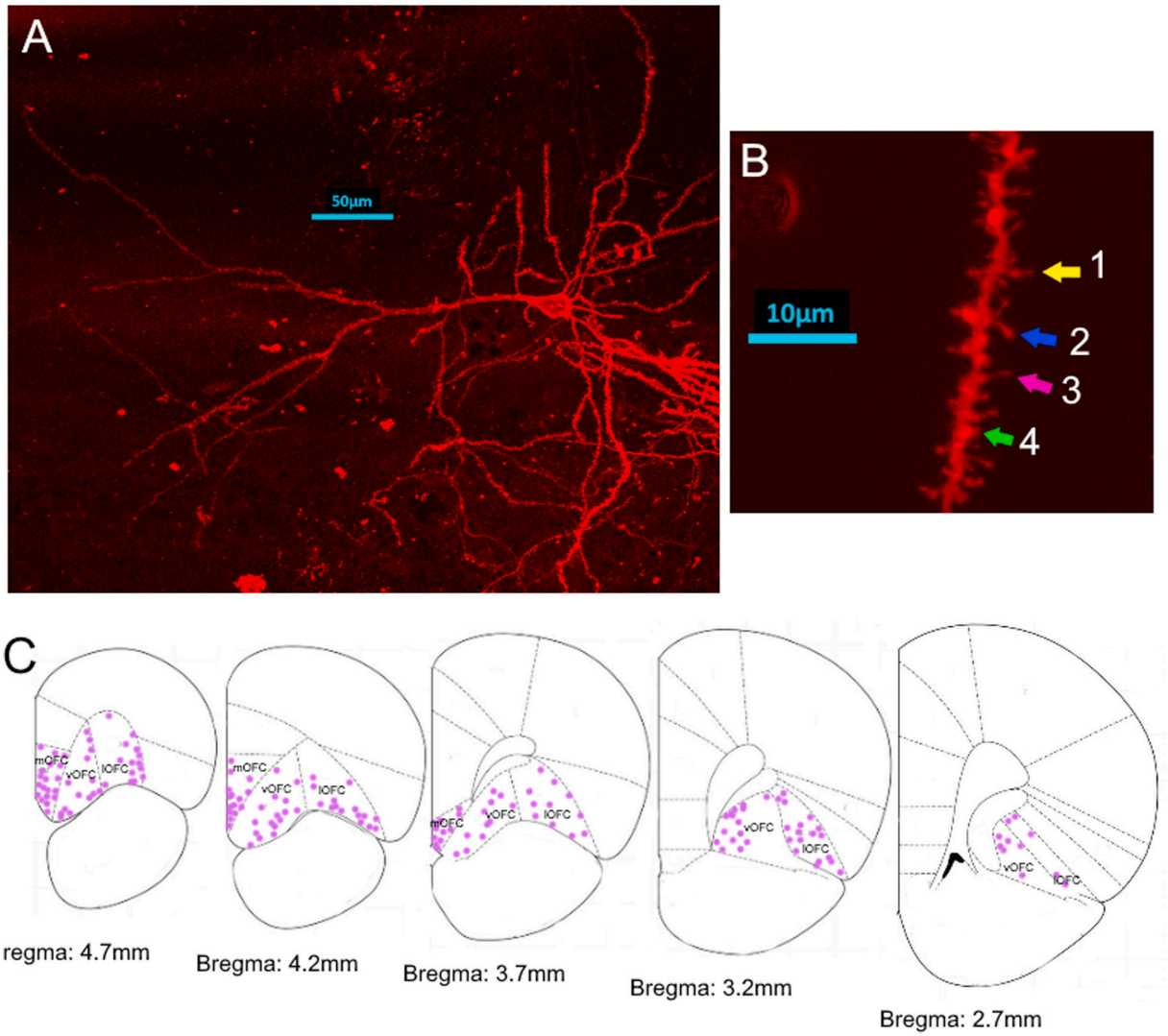

Fig. 6. DiOlistic labelling for Sholl analysis and dendritic spine analysis. A. An OFC neuron in a non-stressed male rat. Scale bar = 50 µm. **B**. An apical dendritic branch of a neuron in the OFC of a non-stressed male rat used for spine density analysis. Arrowheads point out different subtypes of spines. Arrow 1 (yellow): filopodia; arrow 2 (blue): mushroom spine; arrow 3 (pink): thin spine; Arrow 4 (green): stubby spine. Scale bar = 10 µm **C.** Location of DiOlistically labeled neurons analyzed in our experiments (mOFC = medial OFC; vOFC = ventral OFC; lOFC = lateral OFC). (For interpretation of the references to colour in this figure legend, the reader is referred to the Web version of this article.)

"opto-LTP" and "opto-LTD" in this paper to simplify communication. The optical stimulation patterns used were based on electrical LTP and LTD protocols used to induce plasticity in the MDT projection to mouse medial prefrontal cortex (Herry and Garcia, 2002). In so doing, we follow the precedent of Herry and Garcia (2002), who also referred to changes in evoked LFPs recorded in mPFC after high and low frequency stimulation in MDT as LTP and LTD, respectively.

The results of this study showed that optogenetically inducing LTD in the MDT-OFC pathway improved performance on a reversal learning task that had been compromised by stress in rats. Conversely, inducing opto-LTP in the same pathway was sufficient to mimic the stressed-induced deficit in reversal learning. Furthermore, LTP could not be induced in stressed rats, a finding that, considered with the above observations, suggests that CIC stress impairs reversal learning in part by increasing excitability in the OFC. The increase in dendritic elaboration of the medial OFC of stressed rats also lends support for this hypothesis. Modifications in dendritic spine morphology in OFC may in part underlie altered plastic responses after stress.

4.1. Behavioral effects of optogenetic LTD and LTP

We employed a novel optogenetic approach to manipulate neuronal plasticity *in vivo*. The ChETA variant of channelrhodopsin affords fast spike dynamics with reduced artifacts (Gunaydin et al., 2010). After viral induction of ChETA expression in glutamate neurons in the MDT, we successfully generated opto-LTD and opto-LTP to induce bidirectional plasticity in responses evoked in the MDT-OFC pathway. Several crucial controls reinforce the validity of these findings. Rats receiving the opto-LTD or opto-LTP laser stimulation protocol without viral injection did not show any behavioral modifications, indicating that the use of the laser itself does not alter reversal learning. The utilization of a GFP control virus also provided evidence that the process of MDT viral injection and infection alone does not alter reversal learning. Previous work examining the induction of plasticity in OFC has been limited to electrical stimulation in OFC brain slices (Nimitvilai et al., 2016; Zhou et al., 2018), whereas the optogenetic approach permits an *in vivo* investigation of OFC plasticity with pathway specificity.

We focused our attention on the MDT-OFC afferent pathway due to an abundance of evidence implicating these two brain regions in the

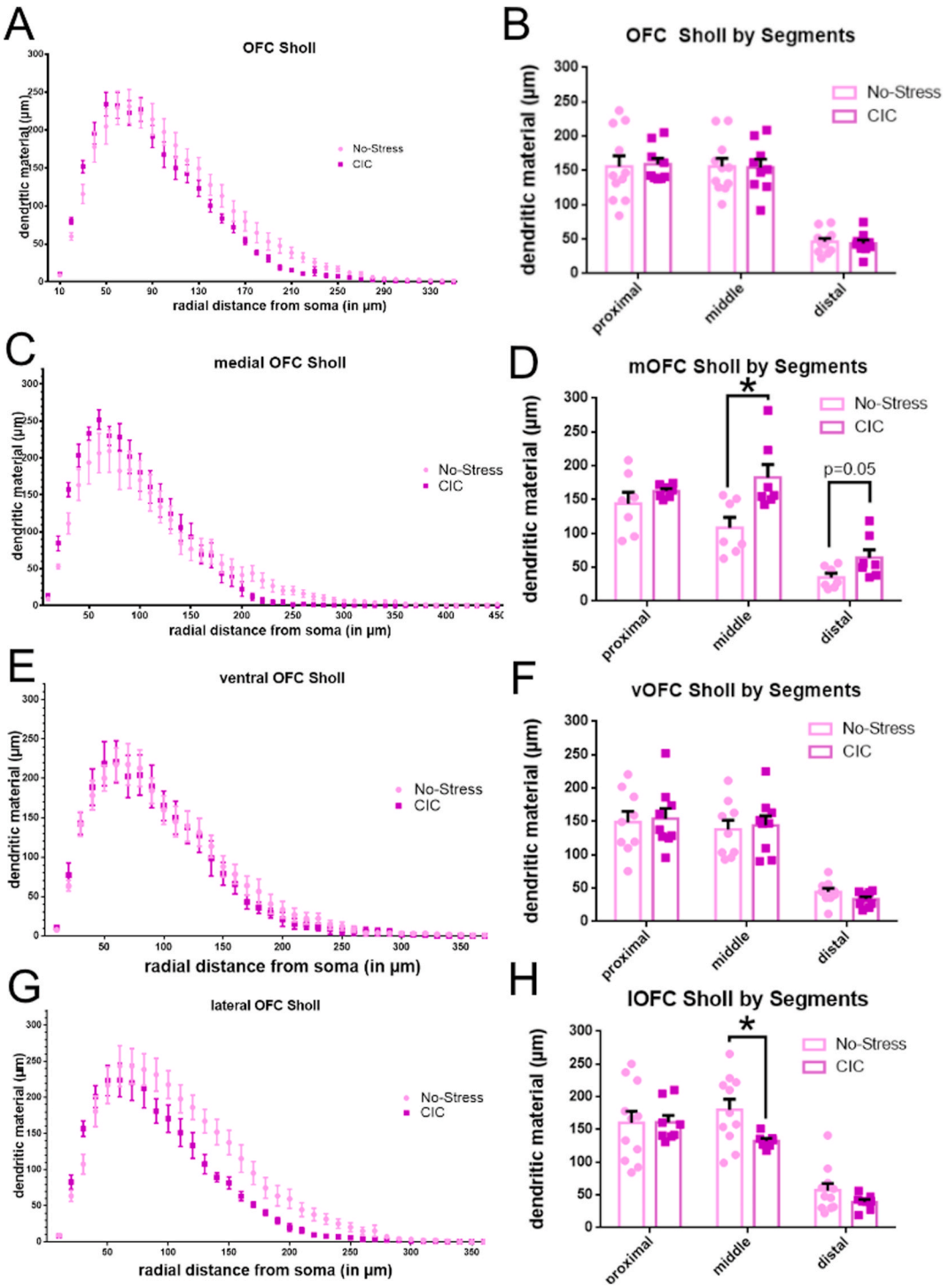

Fig. 7. Sholl analysis of the OFC and its subregions. A. Sholl analysis of the entire OFC (n = 8–11 per group). **B.** Analysis of dendritic material in proximal, middle and distal segments of the dendritic tree of labeled neurons in OFC overall revealed no differences between groups. **C.** Sholl analysis for medial OFC neurons (n = 7 per group). **D.** Analysis of dendritic material in proximal, middle and distal segments of the dendritic tree of labeled neurons in mOFC revealed an increase in middle apical dendritic material after CIC stress (*p < 0.05, *t*-test). **E.** Sholl analysis for ventral OFC neurons (n = 8–10 per group). **F.** Analysis of dendritic material in proximal, middle and distal segments of the dendritic tree of labeled neurons in vOFC revealed no differences between groups. **G.** Sholl analysis for lateral OFC (n = 6–11 per group). **H.** Analysis of dendritic material in proximal, middle and distal segments of the dendritic tree of labeled neurons in lOFC revealed a decrease in middle apical dendritic material after CIC (*p < 0.05, *t*-test). One point was identified as an outlier by the Grubbs Outlier Test and excluded from analysis.

modulation of reversal learning. Several studies have indicated that OFC lesions result in reversal learning impairment in rats (Chudasama and Robbins, 2003; McAlonan and Brown, 2003; Young and Shapiro, 2009), primates (Dias et al., 1996; Izquierdo et al., 2004), and humans (Daum et al., 1991; Rolls et al., 1994). Additionally, MDT lesions also impair reversal learning (Block et al., 2007; Dolleman-van der Weel et al., 2009; Hunt and Aggleton, 1998; Parnaudeau et al., 2013). Several studies confirm the connectivity between these two regions. MDT afferents synapse onto pyramidal neurons in the prefrontal cortex (Négyessy et al., 1998) in both the middle and superficial layers of the cortex (Xiao

Table 1
Effect of CIC on spine morphology.

Region	Thin	Stubby	Mushroom	Filipodia
OFC	No change	No change	No change	↓ after CIC
mOFC	↑ after CIC	No change	↓ after CIC	↓ after CIC
vOFC	No change	No change	No change	↓ after CIC
lOFC	No change	No change	No change	No change

Abbreviations: OFC: orbitofrontal cortex, mOFC: medial orbitofrontal cortex, vOFC: ventral orbitofrontal cortex, lOFC: lateral orbitofrontal cortex, CIC: chronic intermittent cold stress, NS: non-stressed.

Table 2
Effect of sex on spine morphology.

Region	Thin	Stubby	Mushroom	Filipodia
OFC	Female > Male	No difference	No difference	No difference
mOFC	No difference	No difference	NS Male >CIC Male,NS Female,CIC Female	NS Male > CIC Female
vOFC	No difference	No difference	No difference	No difference
lOFC	No difference	No difference	No difference	No difference

Abbreviations: OFC: orbitofrontal cortex, mOFC: medial orbitofrontal cortex, vOFC: ventral orbitofrontal cortex, lOFC: lateral orbitofrontal cortex, CIC: chronic intermittent cold stress, NS: non-stressed.

et al., 2009). Different subregions of the MDT also provide distinct projections to various PFC subregions: the central MDT projects to the OFC, the medial MDT projects to the mPFC, and the lateral MDT projects to the dorsal-medial mPFC (Jones, 2012).

Our focus on recording MDT afferent-evoked responses in the lateral OFC was derived from evidence in the literature that this subregion plays a crucial role in reversal learning. Lateral OFC lesions were sufficient to impair reversal learning (Kim and Ragozzino, 2005), and human subjects exhibit increased activity in lateral OFC during reversal learning (Ghahremani et al., 2010). We have also reported results in several previous studies indicating that direct pharmacological manipulation specifically of the lateral OFC can produce impairments (Donegan et al., 2014) or enhancements (Patton et al., 2017) in reversal learning. Finally, the afferent innervation from the MDT is greater within the lateral OFC than it is in more rostral areas of the OFC, including the medial OFC (Murphy and Deutch, 2018).

Opto-LTP in the MDT-OFC pathway was sufficient to induce a deficit in reversal learning, mimicking the detrimental effect of cold stress. By contrast, opto-LTD in the same pathway corrected the reversal learning deficit induced by CIC stress. This is consistent with our previous observations using ketamine, which depressed evoked responses in the MDT-OFC pathway and also rescued stress-induced reversal learning deficits (Patton et al., 2017). It is also worth noting that inducing opto-LTD in non-stressed control animals appeared to produce a modest deficit in reversal learning, particularly in males, although this trend was not significant (Fig. 4B and C). This would suggest that an optimal range of function is necessary in prefrontal cortical circuits for the successful mediation of complex cognitive processes such as reversal learning. Therefore, disrupting OFC function in either direction in a non-impaired rat may be detrimental. Future experimentation is necessary to explore this in detail.

Changes in MDT afferent-evoked response were recorded in the OFC immediately after optogenetic stimulation of MDT terminals in OFC. In the behavioral experiments, optical stimulation was applied just prior to the reversal learning task. This allowed us to isolate the effects of laser stimulation solely on reversal learning, and not on the acquisition of learned contingencies immediately preceding reversal learning. However, a limitation of this study is that we have not yet determined the duration of the effects of opto-LTP and opto-LTD, either on the potentiation and attenuation, respectively, of afferent-evoked response in OFC, or on behavioral performance on the reversal learning task. Prior studies have revealed that LTP and LTD induction in the dentate gyrus of awake rats persists for weeks (Abraham et al., 1994). Using a different strategy to induce optogenetic potentiation and depression in the dorsomedial striatum, changes in alcohol-seeking behavior were observed to persist for several days (Ma et al., 2018). The literature suggests that alterations in spine morphology can occur within minutes of electrical LTP induction (Matsuzaki et al., 2004) and within 45 min of electrical LTD induction (Zhou et al., 2004), that can persist for months (Trachtenberg et al., 2002) or even years (Grutzendler et al., 2002). Future experiments assessing the duration of alterations in dendritic and spine morphology after stress, and particularly after opto-LTP or opto-LTD stimulation, would help to further establish if there is a link between the structural changes and the functional changes in afferent-evoked response.

We observed an occlusion of LTP in CIC-stressed animals, indicating that CIC may potentiate the thalamic-OFC pathway, making further potentiation difficult. The OFC is not unique in this regard. The basolateral amygdala, another brain region marked by stress-induced hyperexcitability (Sharp, 2017), also exhibits LTP suppression after stress (Kavushansky and Richter-Levin, 2006). Similarly, humans with major depressive disorder have impaired LTP-like plasticity (Kuhn et al., 2016), suggesting that occlusion of LTP after stress may be relevant to the human clinical condition.

The behavioral results seen in the OFC are in contrast to our recent findings in the mPFC (Bulin et al., 2020). Whereas opto-LTP was beneficial to cognitive flexibility in the mPFC, it was detrimental in the OFC, and vice versa for opto-LTD. To further address the functional separation of these PFC subregions, and to confirm regional specificity of the effects seen after optogenetic manipulations in OFC, we induced opto-LTP and opto-LTD in the mPFC and observed no impact on reversal learning. Differences in neuronal encoding between these two subregions may be important to understanding these findings: mPFC neurons track current task rules and guide the behavioral response when rules change, while OFC neurons track outcome value and expectancy and guide the behavioral response to changes in reward contingency (Park and Moghaddam, 2017). Potentiation in the OFC may impair reversal learning because the aberrantly strengthened connections might impede the ability to abandon a previously established stimulus-reward contingency in favor of a newly rewarded alternative. This potentiation of afferent-driven response may make it challenging for OFC neurons to modify their firing patterns to reflect the new contingency, thereby interfering with its ability to signal prediction errors and update changes in value. Likewise, LTD induction immediately preceding reversal learning may weaken these connections, enabling an easier transition to forming a new stimulus-reward contingency.

4.2. *Effects of CIC stress on dendritic morphology and spine composition*

DiOlistic labelling revealed stress-induced changes in neuronal dendritic and spine morphology that may underlie in part the observed behavioral changes. Sholl analysis revealed an increase in dendritic length after stress in the middle dendritic segment of mOFC neurons, but a decrease in the middle segment of lOFC neurons. These regionally-specific changes may reflect the different functional roles of these OFC subdivisions. Medial OFC activity correlates with persevering with current behaviors, while lateral OFC activity correlates with modifying one's behavioral strategy (O'Doherty et al., 2003). Therefore, an increase in mOFC dendritic material may indicate continued rigidity in the face of a changing environment, while a reduction in lOFC dendritic material may suggest a reduction in the ability to change behavioral strategy – both acting to impair reversal learning.

However, given that the attenuation of MDT-evoked response induced by opto-LTD in the lOFC was beneficial to reversal learning impaired by CIC stress, and the increase in response induced by opto-

LTP in lOFC was detrimental to reversal learning, it is puzzling that dendritic length was modestly decreased in lOFC after CIC stress, whereas it was increased in mOFC. One possible explanation for this might be that, rather than causing a reduced response, the modest decrease in dendritic length seen in the lOFC after stress may instead be a compensatory response to a functional increase in afferent-evoked activation in this region. Any such increase in response after stress must then have been mediated by other mechanisms, such as increased trafficking of excitatory receptors to the synapse (Groc et al., 2008). It is also possible that such functional changes in the lateral OFC may have then secondarily induced the structural changes observed in the medial OFC after stress, as these two subregions are interconnected (Carmichael and Price, 1996). Alternatively, the mechanism by which CIC stress impairs reversal learning may be driven by the medial OFC, while the correction of aberrant behavior may be driven by an independent mechanism in the lateral OFC. Both regions are important to reversal learning, but they modulate different aspects of this complex cognitive process, as discussed above. Future studies selectively targeting the mOFC for optogenetic manipulation will help us determine the specific roles of the mOFC and lOFC in stress-induced impairment of reversal learning, and in its rescue by effective intervention.

The changes in dendritic length we observed were only significant in the middle segment of the dendritic arbor, similar to a previous report of increased dendritic length in the middle and distal segments of OFC neurons after stress (Liston et al., 2006). In that study, increases in dendritic length were reported in the agranular insular region of the OFC, which is situated even more laterally than the lOFC. By contrast, we observed an increase in the mOFC, but decreased dendritic length in the lOFC. However, it is noteworthy that the stressor used in that study, repeated prolonged restraint stress, did not produce an impairment in reversal learning. CIC stress is a metabolic stressor. Thus, it would be informative to measure changes in dendritic length in the OFC after another non-metabolic, psychogenic stressor such as chronic unpredictable stress, that also does not produce robust changes in reversal learning (Bulin et al., 2020). Comparing the effects of stressors that impair reversal learning and those that do not can provide insight into whether the observed changes in dendritic morphology have a causal role in the disruption of prefrontal cognition after stress, or if they may instead be correlates of such effects, but are more involved in other aspects of stress pathology.

Few studies have examined changes in spine density or morphology in OFC, and our findings are largely in line with prior reports (McGuier et al., 2015; Muhammad et al., 2012; Whyte et al., 2019). There were no changes in spine density after stress, but there were alterations in spine composition. In general, there was an increase in the proportion of thin spines and a reduction in the proportion of mushroom spines in the OFC after stress. Thin spines are highly labile spines that can rapidly grow or rapidly disappear (Noguchi et al., 2005). Therefore, the overall shift from mature mushroom spines to more labile thin spines in the OFC may signal a disruption of established connections and optimal circuit function necessary for effective reversal learning.

4.3. Translational relevance

This work has potential translational relevance, as the OFC plays an important role in the pathology of many stress-related psychiatric illnesses. Recent clinical studies have utilized deep transcranial magnetic stimulation to treat depression (Levkovitz et al., 2015) and schizophrenia (Linsambarth et al., 2019). This approach uses high-frequency stimulation over the prefrontal cortex, and has resulted in significant symptom improvement. However, stimulating the prefrontal cortex nonspecifically, as a homogenous unit, may result in unexpected side effects as a result of off-target potentiation of related prefrontal circuits. Additionally, low frequency repetitive transcranial magnetic stimulation over the OFC has proven effective in treating OCD (Ruffini et al., 2009). Together, our results suggest that stimulation-induced plasticity may be a potential mechanism underlying the therapeutic benefits of such treatments in improving cognitive flexibility in stress-related psychiatric disorders.

Conflicts of interest

The authors declare that there is no conflict of interest regarding the publication of this paper.

CRediT authorship contribution statement

Samantha M. Adler: Conceptualization, Methodology, Validation, Formal analysis, Investigation, Data curation, Writing - original draft, Writing - review & editing, Visualization. **Milena Girotti:** Conceptualization, Methodology, Validation, Formal analysis, Investigation, Writing - review & editing, Visualization. **David A. Morilak:** Conceptualization, Methodology, Validation, Resources, Writing - review & editing, Supervision, Project administration, Funding acquisition.

Acknowledgements

Thanks to Dr. Sarah Bulin for providing technical expertise and advice in the conduct of these experiments. This work was supported by National Institutes of Mental Health Grant R01 MH053851, National Institutes of Health Training Grant T32 NS082145, and a pilot project grant from the Center for Biomedical Neuroscience, UTHSCSA.

Appendix A. Supplementary data

Supplementary data to this article can be found online at https://doi.org/10.1016/j.ynstr.2020.100258.

References

Abraham, W.C., Christie, B.R., Logan, B., Lawlor, P., Dragunow, M., 1994. Immediate early gene expression associated with the persistence of heterosynaptic long-term depression in the hippocampus. Proc. Natl. Acad. Sci. U. S. A. 91, 10049–10053.
Adler, S.M., Bulin, S.E., Girotti, M., Morilak, D.A., 2018. Stress Effects on Neuronal Connectivity in the Orbitofrontal Cortex Society for Neuroscience, San Diego, CA. Program No. 317.02.
Adler, S.M., Girotti, M., Morilak, D.A., 2019. Stress Effects on Neuronal Connectivity in the Orbitofrontal Cortex. Society for Neuroscience, Chicago, IL. Program No. 322.05.
Baxter, L.R., Schwartz, J.M., Phelps, M.E., Mazziotta, J.C., Guze, B.H., Selin, C.E., Gerner, R.H., Sumida, R.M., 1989. Reduction of prefrontal cortex glucose metabolism common to three types of depression. Arch. Gen. Psychiatr. 46, 243–250.
Beck, A.T., 2008. The evolution of the cognitive model of depression and its neurobiological correlates. Am. J. Psychiatr. 165, 969–977.
Birrell, J.M., Brown, V.J., 2000. Medial frontal cortex mediates perceptual attentional set shifting in the rat. J. Neurosci. 20, 4320–4324.
Block, A.E., Dhanji, H., Thompson-Tardif, S.F., Floresco, S.B., 2007. Thalamic–prefrontal cortical–ventral striatal circuitry mediates dissociable components of strategy set shifting. Cerebr. Cortex 17, 1625–1636.
Bondi, C.O., Rodriguez, G., Gould, G.G., Frazer, A., Morilak, D.A., 2008. Chronic unpredictable stress induces a cognitive deficit and anxiety-like behavior in rats that is prevented by chronic antidepressant drug treatment. Neuropsychopharmacology 33, 320–331.
Bulin, S.E., Hohl, K.M., Paredes, D., Silva, J.D., Morilak, D.A., 2020. Bidirectional optogenetically-induced plasticity of evoked responses in the rat medial prefrontal cortex can impair or enhance cognitive set-shifting. eNeuro 7. ENEURO.0363-19.
Carmichael, S.T., Price, J.L., 1996. Connectional networks within the orbital and medial prefrontal cortex of macaque monkeys. J. Comp. Neurol. 371, 179–207.
Castaneda, A.E., Tuulio-Henriksson, A., Marttunen, M., Suvisaari, J., Lönnqvist, J., 2008. A review on cognitive impairments in depressive and anxiety disorders with a focus on young adults. J. Affect. Disord. 106, 1–27.
Chudasama, Y., Robbins, T.W., 2003. Dissociable contributions of the orbitofrontal and infralimbic cortex to pavlovian autoshaping and discrimination reversal learning: further evidence for the functional heterogeneity of the rodent frontal cortex. J. Neurosci. 23, 8771–8780.
Danet, M., Lapiz-Bluhm, S., Morilak, D.A., 2010. A cognitive deficit induced in rats by chronic intermittent cold stress is reversed by chronic antidepressant treatment. Int. J. Neuropsychopharmacol. 13, 997–1009.
Daum, I., Schugens, M.M., Channon, S., Polkey, C.E., Gray, J.A., 1991. T-maze discrimination and reversal learning after unilateral temporal or frontal lobe lesions in man. Cortex 27, 613–622.

Dias, R., Robbins, T.W., Roberts, A.C., 1996. Primate analogue of the Wisconsin card sorting test: effects of excitotoxic lesions of the prefrontal cortex in the marmoset. Behav. Neurosci. 110, 872–886.
Dolleman-van der Weel, M.J., Morris, R.G.M., Witter, M.P., 2009. Neurotoxic lesions of the thalamic reuniens or mediodorsal nucleus in rats affect non-mnemonic aspects of watermaze learning. Brain Struct. Funct. 213, 329–342.
Donegan, J.J., Girotti, M., Weinberg, M.S., Morilak, D.A., 2014. A novel role for brain interleukin-6: facilitation of cognitive flexibility in rat orbitofrontal cortex. J. Neurosci. 34, 953–962.
Drevets, W.C., 2000. Functional anatomical abnormalities in limbic and prefrontal cortical structures in major depression. In: Progress in Brain Research, 126. Elsevier, pp. 413–431.
Ghahremani, D.G., Monterosso, J., Jentsch, J.D., Bilder, R.M., Poldrack, R.A., 2010. Neural components underlying behavioral flexibility in human reversal learning. Cerebr. Cortex 20, 1843–1852.
Groc, L., Choquet, D., Chaouloff, F., 2008. The stress hormone corticosterone conditions AMPAR surface trafficking and synaptic potentiation. Nat. Neurosci. 11, 868–870.
Grutzendler, J., Kasthuri, N., Gan, W.-B., 2002. Long-term dendritic spine stability in the adult cortex. Nature 420, 812–816.
Gunaydin, L.A., Yizhar, O., Berndt, A., Sohal, V.S., Deisseroth, K., Hegemann, P., 2010. Ultrafast optogenetic control. Nat. Neurosci. 13, 387–392.
Herry, C., Garcia, R., 2002. Prefrontal cortex long-term potentiation, but not long-term depression, is associated with the maintenance of extinction of learned fear in mice. J. Neurosci. 22, 577–583.
Hunt, P.R., Aggleton, J.P., 1998. Neurotoxic lesions of the dorsomedial thalamus impair the acquisition but not the performance of delayed matching to place by rats: a deficit in shifting response rules. J. Neurosci. 18, 10045–10052.
Izquierdo, A., Suda, R.K., Murray, E.A., 2004. Bilateral orbital prefrontal cortex lesions in rhesus monkeys disrupt choices guided by both reward value and reward contingency. J. Neurosci. 24, 7540–7548.
Jones, E.G., 2012. The Thalamus. Springer Science & Business Media.
Kavushansky, A., Richter-Levin, G., 2006. Effects of stress and corticosterone on activity and plasticity in the amygdala. J. Neurosci. Res. 84, 1580–1587.
Kim, J., Ragozzino, M.E., 2005. The involvement of the orbitofrontal cortex in learning under changing task contingencies. Neurobiol. Learn. Mem. 83, 125–133.
Kuhn, M., Mainberger, F., Feige, B., Maier, J.G., Mall, V., Jung, N.H., Reis, J., Klöppel, S., Normann, C., Nissen, C., 2016. State-dependent partial occlusion of cortical LTP-like plasticity in major depression. Neuropsychopharmacology 41, 1521–1529.
Lapiz-Bluhm, M.D., Soto-Pina, A.E., Hensler, J.G., Morilak, D.A., 2009. Chronic intermittent cold stress and serotonin depletion induce deficits of reversal learning in an attentional set-shifting test in rats. Psychopharmacology 202, 329–341.
Levkovitz, Y., Isserles, M., Padberg, F., Lisanby, S.H., Bystritsky, A., Xia, G., Tendler, A., Daskalakis, Z.J., Winston, J.L., Dannon, P., Hafez, H.M., Reti, I.M., Morales, O.G., Schlaepfer, T.E., Hollander, E., Berman, J.A., Husain, M.M., Sofer, U., Stein, A., Adler, S., Deutsch, L., Deutsch, F., Roth, Y., George, M.S., Zangen, A., 2015. Efficacy and safety of deep transcranial magnetic stimulation for major depression: a prospective multicenter randomized controlled trial. World Psychiatr. 14, 64–73.
Li, N., Lee, B., Liu, R.J., Banasr, M., Dwyer, J.M., Iwata, M., Li, X.Y., Aghajanian, G., Duman, R.S., 2010. mTOR-dependent synapse formation underlies the rapid antidepressant effects of NMDA antagonists. Science 329, 959–964.
Linsambarth, S., Jeria, A., Avirame, K., Todder, D., Riquelme, R., Stehberg, J., 2019. Deep transcranial magnetic stimulation for the treatment of negative symptoms in schizophrenia: beyond an antidepressant effect. J. ECT 35, e46–e54.
Liston, C., Miller, M.M., Goldwater, D.S., Radley, J.J., Rocher, A.B., Hof, P.R., Morrison, J.H., McEwen, B.S., 2006. Stress-induced alterations in prefrontal cortical dendritic morphology predict selective impairments in perceptual attentional set-shifting. J. Neurosci. 26, 7870–7874.
Lüscher, C., Nicoll, R.A., Malenka, R.C., Muller, D., 2000. Synaptic plasticity and dynamic modulation of the postsynaptic membrane. Nat. Neurosci. 3, 545–550.
Ma, T., Cheng, Y., Roltsch Hellard, E., Wang, X., Lu, J., Gao, X., Huang, C.C.Y., Wei, X.-Y., Ji, J.-Y., Wang, J., 2018. Bidirectional and long-lasting control of alcohol-seeking behavior by corticostriatal LTP and LTD. Nat. Neurosci. 21, 373–383.
Malenka, R.C., Bear, M.F., 2004. LTP and LTD: an embarrassment of riches. Neuron 44, 5–21.
Matsuzaki, M., Honkura, N., Ellis-Davies, G.C., Kasai, H., 2004. Structural basis of long-term potentiation in single dendritic spines. Nature 429, 761–766.
McAlonan, K., Brown, V.J., 2003. Orbital prefrontal cortex mediates reversal learning and not attentional set shifting in the rat. Behav. Brain Res. 146, 97–103.
McGuier, N.S., Padula, A.E., Lopez, M.F., Woodward, J.J., Mulholland, P.J., 2015. Withdrawal from chronic intermittent alcohol exposure increases dendritic spine density in the lateral orbitofrontal cortex of mice. Alcohol 49, 21–27.
Muhammad, A., Carroll, C., Kolb, B., 2012. Stress during development alters dendritic morphology in the nucleus accumbens and prefrontal cortex. Neuroscience 216, 103–109.
Murphy, M.J.M., Deutch, A.Y., 2018. Organization of afferents to the orbitofrontal cortex in the rat. J. Comp. Neurol. 526, 1498–1526.
Négyessy, L., Hámori, J., Bentivoglio, M., 1998. Contralateral cortical projection to the mediodorsal thalamic nucleus: origin and synaptic organization in the rat. Neuroscience 84, 741–753.
Nimitvilai, S., Lopez, M.F., Mulholland, P.J., Woodward, J.J., 2016. Chronic intermittent ethanol exposure enhances the excitability and synaptic plasticity of lateral orbitofrontal cortex neurons and induces a tolerance to the acute inhibitory actions of ethanol. Neuropsychopharmacology 41, 1112–1127.
Noguchi, J., Matsuzaki, M., Ellis-Davies, G.C., Kasai, H., 2005. Spine-neck geometry determines NMDA receptor-dependent Ca2+ signaling in dendrites. Neuron 46, 609–622.
O'Doherty, J.P., Dayan, P., Friston, K., Critchley, H., Dolan, R.J., 2003. Temporal difference models and reward-related learning in the human brain. Neuron 38, 329–337.
Park, J., Moghaddam, B., 2017. Impact of anxiety on prefrontal cortex encoding of cognitive flexibility. Neuroscience 345, 193–202.
Parnaudeau, S., O'Neill, P.-K., Bolkan, S.S., Ward, R.D., Abbas, A.I., Roth, B.L., Balsam, P. D., Gordon, J.A., Kellendonk, C., 2013. Inhibition of mediodorsal thalamus disrupts thalamofrontal connectivity and cognition. Neuron 77, 1151–1162.
Patton, M.S., Lodge, D.J., Morilak, D.A., Girotti, M., 2017. Ketamine corrects stress-induced cognitive dysfunction through JAK2/STAT3 signaling in the orbitofrontal cortex. Neuropsychopharmacology 42, 1220–1230.
Raio, C.M., Hartley, C.A., Orederu, T.A., Li, J., Phelps, E.A., 2017. Stress attenuates the flexible updating of aversive value. Proc. Natl. Acad. Sci. Unit. States Am. 114, 11241–11246.
Rolls, E.T., Hornak, J., Wade, D., McGrath, J., 1994. Emotion-related learning in patients with social and emotional changes associated with frontal lobe damage. J. Neurol. Neurosurg. Psychiatr. 57, 1518–1524.
Ruffini, C., Locatelli, M., Lucca, A., Benedetti, F., Insacco, C., Smeraldi, E., 2009. Augmentation effect of repetitive transcranial magnetic stimulation over the orbitofrontal cortex in drug-resistant obsessive-compulsive disorder patients: a controlled investigation. Prim. Care Companion J. Clin. Psychiatry 11, 226–230.
Sharp, B.M., 2017. Basolateral amygdala and stress-induced hyperexcitability affect motivated behaviors and addiction. Transl. Psychiatry 7, e1194.
Shilyansky, C., Williams, L.M., Gyurak, A., Harris, A., Usherwood, T., Etkin, A., 2016. Effect of antidepressant treatment on cognitive impairments associated with depression: a randomised longitudinal study. The Lancet Psychiatry 3, 425–435.
Trachtenberg, J.T., Chen, B.E., Knott, G.W., Feng, G., Sanes, J.R., Welker, E., Svoboda, K., 2002. Long-term in vivo imaging of experience-dependent synaptic plasticity in adult cortex. Nature 420, 788–794.
Whyte, A.J., Kietzman, H.W., Swanson, A.M., Butkovich, L.M., Barbee, B.R., Bassell, G.J., Gross, C., Gourley, S.L., 2019. Reward-related expectations trigger dendritic spine plasticity in the mouse ventrolateral orbitofrontal cortex. J. Neurosci. 39, 4595–4605.
Xiao, D., Zikopoulos, B., Barbas, H., 2009. Laminar and modular organization of prefrontal projections to multiple thalamic nuclei. Neuroscience 161, 1067–1081.
Young, J.J., Shapiro, M.L., 2009. Double dissociation and hierarchical organization of strategy switches and reversals in the rat PFC. Behav. Neurosci. 123, 1028–1035.
Zhou, L., Fisher, M.L., Cole, R.D., Gould, T.J., Parikh, V., Ortinski, P.I., Turner, J.R., 2018. Neuregulin 3 signaling mediates nicotine-dependent synaptic plasticity in the orbitofrontal cortex and cognition. Neuropsychopharmacology 43, 1343–1354.
Zhou, Q., Homma, K.J., Poo, M.-m., 2004. Shrinkage of dendritic spines associated with long-term depression of hippocampal synapses. Neuron 44, 749–757.